



ELSEVIER

Earth and Planetary Science Letters 178 (2000) 139–149

EPSL

www.elsevier.com/locate/epsl

Lithosphere structure beneath the Phanerozoic intracratonic basins of North America

Edouard Kaminski, Claude Jaupart*

Institut de Physique du Globe de Paris, 4 Place Jussieu, 75252 Paris Cedex 5, France

Received 3 August 1999; received in revised form 4 February 2000; accepted 19 February 2000

Abstract

Four intracratonic basins of North America, the Hudson Bay, Michigan, Illinois and Williston basins, have similar ages and are close to one another. Yet, they exhibit different subsidence histories characterised by different time-scales and sediment thicknesses. They can be explained by local lithosphere thinning and by the cooling of the induced thermal anomaly. Within the framework of 1D thermal models for vertical heat transport, each basin requires a different lithosphere thickness or a different boundary condition at the base of the lithosphere. Heat flow and seismic studies show that, beneath the North American craton, the lithosphere is too thick for the assumption of purely vertical heat transfer to be valid. Thermal models are developed to account for finite thermal anomaly width and for two types of basal boundary conditions, fixed temperature or fixed heat flux. Different subsidence histories are explained by deep lithospheric anomalies of different sizes. The stability of thick continental roots requires the mantle part of the lithosphere to be compositionally buoyant with respect to ‘normal’ convecting mantle. Localised lithospheric thinning, due for example to plume penetration, results in the emplacement of compositionally denser mantle into the lithosphere. This represents a load which drives permanent flexure. The cooling time and the characteristics of flexure allow constraints on the dimensions of these deep lithospheric anomalies. There are no solutions for lithosphere thicknesses less than 170 km. The Williston and Illinois basins are associated with wide (~ 200 km) and thin anomalies (~ 100 km), whereas the Michigan and Hudson Bay are located on top of narrow (~ 100 km) and tall (~ 200 km) anomalies. © 2000 Elsevier Science B.V. All rights reserved.

Keywords: lithosphere; intracratonic basins; North America; Phanerozoic; thermal anomalies; one-dimensional models

1. Introduction

There is considerable debate about the structure of the continental lithosphere and estimates of its thickness vary within a large range of about 120–

400 km [1–4]. These estimates have been obtained using different geophysical techniques and correspond to different features of the boundary layer at the top of the convecting mantle. For example, the downward extrapolation of crustal geotherms deal with the upper part where heat transport occurs by conduction, whereas seismic models provide constraints on the whole boundary layer, which, by definition, is thicker. An alternative method is to use the time-dependent behaviour of continental lithosphere following a thermal

* Corresponding author. Tel.: +33-1-4427-6873;
Fax: +33-1-4427-2481; E-mail: cj@ccr.jussieu.fr

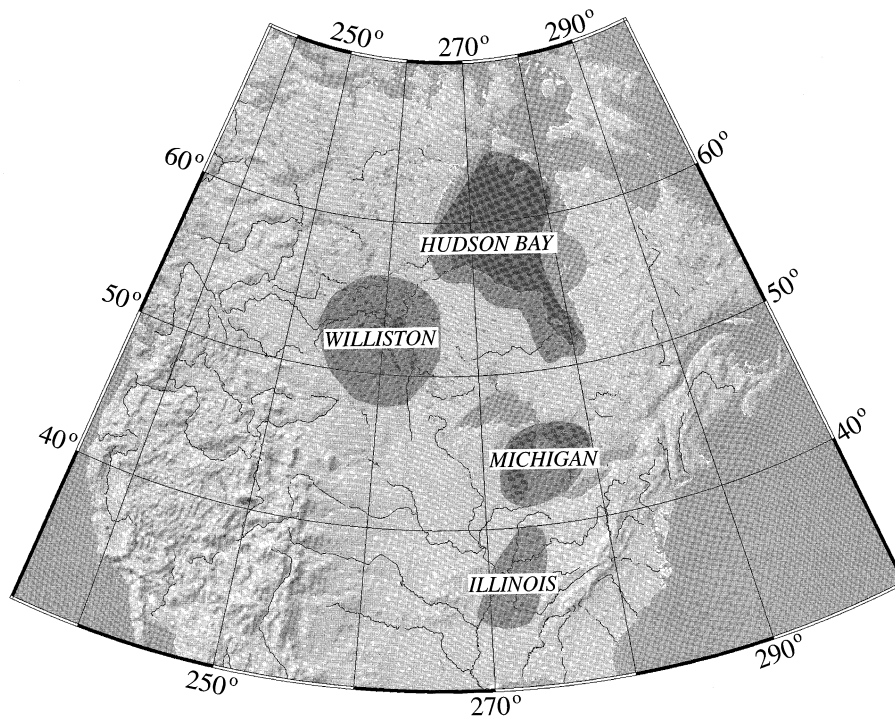


Fig. 1. Four Phanerozoic intracratonic basins of North America: Hudson Bay, Illinois, Michigan and Williston.

perturbation, which is sensitive to thickness. Such transients have been studied using the subsidence of intracratonic basins located away from active plate boundaries [4–6].

In North America, it has been proposed that the thickness of the continental lithosphere is about 115 km beneath the Michigan basin and 270 km beneath the Williston [4,6]. For two basins of similar age located on the same Precambrian continent, such a large difference is surprising. This motivated Hamdani et al. [7,8] to investigate the influence of thermal boundary conditions at the base of the lithosphere. They showed that subsidence is slower for a fixed flux than for a fixed temperature and hence attributed different subsidence behaviours to different thermal processes at depth. However, they provided no explanation for such differences. All these studies rely on 1D thermal models for purely vertical heat transfer and hence require an anomaly of horizontal extent much larger than the lithosphere thickness. The Michigan and Williston basins have been attributed to a large part to plate

flexure driven by a deep load [4–6,9]. This load is related to the initial thermal anomaly and has a radius of about 120 km beneath the Michigan basin [4], which is smaller than the thickness of the lithosphere beneath the North American craton [10–12]. Under these conditions, the assumption of purely vertical heat transfer is not tenable and the thermal models must be reevaluated.

In this paper, we study the behaviour of the lithosphere following a deep thermal event, such that part of the lithosphere is replaced by mantle material from below. We account for the finite lateral extent of the thermal anomaly. We use thermal and flexural models to determine the dimensions and density of the new material incorporated into the lithosphere beneath four intracratonic basins of North America, the Hudson Bay, Michigan, Illinois and Williston basins. These basins are of similar age and are located on lithospheres of similar age and composition (Fig. 1). Subsidence data are available for all of them (Fig. 2 and Table 1). The analysis leads to constraints on lithosphere thickness. The results

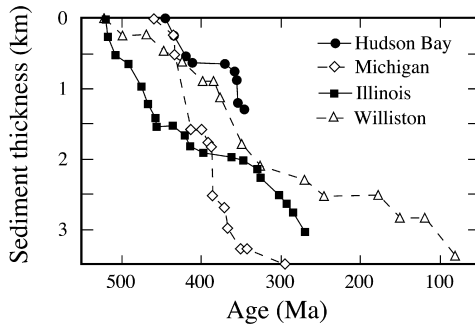


Fig. 2. Evolution of sedimentation in four intracratonic basins of North America (see Table 1 for references). In the Williston, a late phase of sedimentation starting at about 100 Ma is attributed to western Canadian foreland subsidence.

are discussed in terms of the physical mechanisms responsible for basin formation.

2. The intracratonic basins of North America

2.1. Subsidence mechanisms

Beneath each basin, the present-day sedimentary infill requires a permanent load to drive lithosphere flexure. For such old basins, thermal anomalies have long decayed away and hence the load must have a compositional origin. One possibility is that there has been an episode of uplift before subsidence, leading to erosion and hence to a local reduction of crustal thickness. However, there is no evidence for significant crustal thinning beneath the Williston and Michigan basins [17,18]. One alternative is to invoke crustal metamorphism. Several reactions with different density changes have been used: gabbro to eclogite, greenschist to amphibolite and gabbro to garnet–granulite [4,8,9]. However, the extreme

heterogeneity of crustal assemblages [19] implies that only part of the crust has the right starting composition and may undergo the phase change. The average density increase is smaller than postulated by an unknown amount, which makes this subsidence mechanism difficult to test. Direct verification requires detailed knowledge of crustal structure beneath the basins, which is not available [13].

The Michigan basin provides a good example of the problems encountered when setting up a physical model for subsidence. An early short-lived phase of subsidence started at about 520 Ma and lasted for about 20 Myr only. Sedimentation was interrupted for about 60 Myr before the onset of the major phase which led to the accumulation of more than 3 km of strata. The first subsidence phase has been attributed to crustal metamorphism activated by a deep heating event and the second one to the ensuing thermal relaxation [20,9]. However, this model cannot be applied to the neighbouring Illinois basin, where there has been no interruption of subsidence. In fact, the two subsidence phases of the Michigan basin correspond to separate events because they are also recorded on distant continental margins [5].

In this study, we propose a single framework to account for both subsidence and emplacement of a permanent load. To generate a thermal anomaly in the deep lithosphere, one must invoke the penetration of a mantle plume, a delamination event or some form of deep stretching. In all cases, a volume of lithosphere is replaced by mantle material from below. It is now established that the continental lithosphere is thick and colder than the surrounding mantle, which requires a compositional contrast between the two [1,21]. Thus, the

Table 1
Data for four intracratonic basins of North America

Parameter	Hudson Bay	Michigan	Williston	Illinois
Total sediment thickness, w_0 (km)	1.3	3.4	3.4	3.0
Flexural parameter, γ (km)	≈ 130	90	130	≈ 90
Time for 90% subsidence, τ_{90} (Myr)	100	110	420	240
Point load, Q_0 ($\times 10^{18}$ N)	1.2	1.5	3.1	1.3

Subsidence data are extracted from [5,13,14]. Flexural parameters for Michigan and Williston from [6,9]. For Illinois and Hudson, the flexural parameter is evaluated from the equivalent radius in the structural maps given in [15,16].

new lithospheric material is both hotter and compositionally denser than the material it replaces. With time, the thermal anomaly disappears due to diffusion, but the compositional anomaly remains and hence the net result is a permanent load responsible for subsidence. Thermal and compositional effects are directly related and the observations can be used to characterise the deep lithospheric anomalies required beneath the basins. In turn, these results may be used to assess plausible mechanisms for intracratonic basin formation.

2.2. Parameters extracted from the subsidence record

The relaxation of a thermal perturbation is a realistic mechanism for subsidence over large times, but a detailed fit to the preserved sedimentary record involves many additional effects, such as global sea level variations and tectonic events, some of which are ill-constrained [22]. We take a simpler approach and extract two parameters from the sedimentary record (Table 1): the duration of subsidence, which characterises thermal relaxation, and the total sediment thickness, which is related to a permanent load at depth. In order to compare the different cooling histories, we define subsidence duration by the time needed to achieve 90% of the final subsidence, denoted by τ_{90} . Sediment thicknesses are extracted from previous studies (Table 1). For the Williston basin, following [6], we do not take into account a recent widespread episode of carbonate sedimentation. For the Michigan basin, we focus on the major subsidence phase starting at 460 Ma, as in [5].

2.3. Lithosphere flexure

We consider permanent lithosphere flexure due to a deep disk load of radius a and hence do not account for transient effects associated with creep in the lower lithosphere [5]. We use the classical thin elastic plate model [23,4], which introduces the flexural parameter, γ :

$$\gamma = \left[\frac{Eh^3}{12(1-\nu^2)\Delta\rho_s g} \right]^{1/4} \quad (1)$$

where h is the elastic thickness of lithosphere, E is the bulk modulus, ν is Poisson's ratio and g is the acceleration of gravity. In this equation, $\Delta\rho_s = \rho_m - \rho_s$, where ρ_m is the mantle density at the Moho, set to 3300 kg m^{-3} , and ρ_s is the average sediment density. For a uniform load, P_o , applied between $r=0$ and $r=a$, the plate vertical deflexion w is [23]:

$$r < a, \quad w(r) = \frac{P_o}{\Delta\rho_s g} \left[\frac{a}{\gamma} \text{ker}'\left(\frac{r}{\gamma}\right) \text{ber} \left(\frac{r}{\gamma}\right) - \frac{a}{\gamma} \text{kei}'\left(\frac{r}{\gamma}\right) \text{bei} \left(\frac{r}{\gamma}\right) + 1 \right] \quad (2)$$

$$r > a, \quad w(r) = \frac{P_o}{\Delta\rho_s g} \left[\frac{a}{\gamma} \text{ber}'\left(\frac{r}{\gamma}\right) \text{ker} \left(\frac{r}{\gamma}\right) - \frac{a}{\gamma} \text{bei}'\left(\frac{r}{\gamma}\right) \text{kei} \left(\frac{r}{\gamma}\right) \right] \quad (3)$$

where ker , ber , kei and bei are Kelvin–Thomson functions [24, p. 383].

The amplitude of flexure is proportional to P_o . Scaling the local sediment thickness, $w(r)$, by the maximum thickness at the centre leads to a dimensionless basin shape which depends only on ratio a/γ . The basin shape is almost the same as that for a point-load for values smaller than about 1.2. For larger values of a/γ , the basin develops a flat floor which is not consistent with the observations, as will be shown below. We shall thus use the constraint that a/γ is less than 1.2. In this case, the basin width is approximately eight times the flexural parameter [4]. We have used this relationship for the Illinois and Hudson Bay basins. For the Williston and Michigan basins, we have taken the values of the flexural parameter at the end of subsidence given in [6,9].

For given sediment density, values of sediment thickness and basin width only allow an estimate of the equivalent point load, $Q_o = \pi a^2 P_o$. The average density of the Michigan basin sedimentary strata is well constrained [25] at the value of 2610 kg m^{-3} and we have adopted it for all basins. Our values of Q_o are slightly smaller than those of previous authors who used a smaller sediment density of 2500 kg m^{-3} [4,6]. For a de-

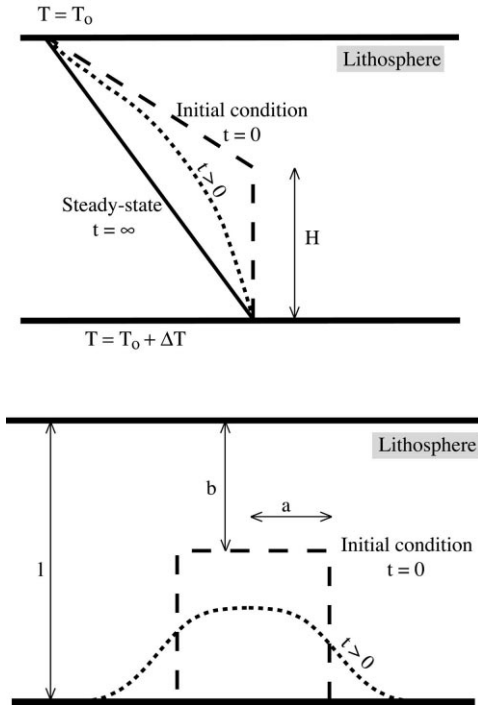


Fig. 3. Schematic representation of the lithosphere and of the deep temperature anomaly at different stages of cooling.

tailed flexure analysis, one must specify the anomaly radius a , which will be obtained from a thermal model.

3. Thermal model for subsidence

3.1. Basic equations

We consider a lithosphere of thickness l with a cylindrical thermal anomaly of radius a between depths l and b (Fig. 3). At the surface ($z=0$), the temperature is fixed at T_0 . At steady-state, the base of the lithosphere is at $T=T_0+\Delta T$. We assume that the thermally perturbed region is at a uniform temperature $T_0+\Delta T$. We write temperature as the sum of the equilibrium temperature and a dimensionless perturbation:

$$T(r, z, t) = T_0 + \Delta T \left[\frac{z}{l} + \theta(r, z, t) \right] \quad (4)$$

where r is the radial distance. θ is a solution of the

heat diffusion equation and we scale time using the vertical diffusion time-scale:

$$\tau = \frac{l^2}{\kappa} \quad (5)$$

where κ is thermal diffusivity (set at $10^{-6} \text{ m}^2 \text{ s}^{-1}$). Dimensionless variables are $t^* = t/\tau$, $z^* = z/l$, $r^* = r/a$ and the anomaly dimensions define two dimensionless numbers:

$$\zeta = \frac{b}{l}, \quad \xi = \frac{a}{l} \quad (6)$$

Temperature is fixed at the top of the lithosphere. At the base, we consider either a fixed temperature or a fixed heat flux. Thermal perturbations are required to vanish at large radial distances.

3.2. 1D solution $\theta_Z(z^*, t^*)$

The initial condition is such that:

$$\theta_Z(z^*, 0) = z^* \left(\frac{1}{\zeta} - 1 \right), \quad \text{for } z^* \leq \zeta \quad (7)$$

$$\theta_Z(z^*, 0) = 1 - z^*, \quad \text{for } z^* \geq \zeta \quad (8)$$

For fixed basal temperature, $\theta_Z(1, t^*) = 0$, the solution is [26, p. 94]:

$$\theta_Z(z^*, t^*) =$$

$$\sum_{n=1}^{\infty} \frac{2}{\zeta (n\pi)^2} \sin(n\pi\zeta) \sin(n\pi z^*) \exp(-n^2\pi^2 t^*) \quad (9)$$

which shows that the time-scale for thermal decay is $\tau_T = l^2/\pi^2\kappa$. For fixed heat flux at the base, $\partial\theta_Z/\partial z^*(1, t^*) = 0$, the solution is [26, p. 113]:

$$\theta_Z(z^*, t^*) = \sum_{n=0}^{\infty} \frac{2}{\left(\frac{2n+1}{2}\pi\right)^2} \left[\frac{\sin\left(\frac{2n+1}{2}\pi\zeta\right)}{\zeta} - (-1)^n \right] \sin\left(\frac{2n+1}{2}\pi z^*\right) \exp\left[-\left(\frac{2n+1}{2}\right)^2 \pi^2 t^*\right] \quad (10)$$

for which the proper time-scale is $\tau_Q = 4l^2/\pi^2\kappa = 4\tau_T$. Cooling and subsidence are much slower than

in the previous case because heat is continuously brought into the lithosphere.

Subsidence is proportional to the amount of contraction in the lithosphere. The final, and total, amount of contraction, S_o , is:

$$S_o = \alpha \Delta T l \int_0^1 \theta(z^*, 0) dz^* = \alpha \Delta T l \frac{1-\zeta}{2} \quad (11)$$

with α the coefficient of thermal expansion. The dimensionless subsidence, $S^*(t^*) = S(t^*)/S_o$, is:

$$S^*(t^*) = \frac{\alpha \Delta T l \int_0^1 [\theta(z^*, 0) - \theta(z^*, t^*)] dz^*}{S_o} = 1 - \frac{2}{1-\zeta} \int_0^1 \theta(z^*, t^*) dz^* \quad (12)$$

The solution depends weakly on the anomaly depth, ζ . Fig. 4 shows the ratio between values of subsidence time τ_{90} for anomalies at the base of the lithosphere ($\zeta=1$) and extending to depth ζ . For fixed temperature boundary conditions, the thermal anomaly gets dissipated at similar rates through the top and bottom. The closer the anomaly is to one of the boundaries, the larger is the heat loss and hence the faster is thermal relaxation. For fixed basal heat flux, the anomaly decays only through heat loss at the top. For increasing ζ , the anomaly is increasingly farther from the top and hence the cooling time increases.

Observed variations of subsidence time

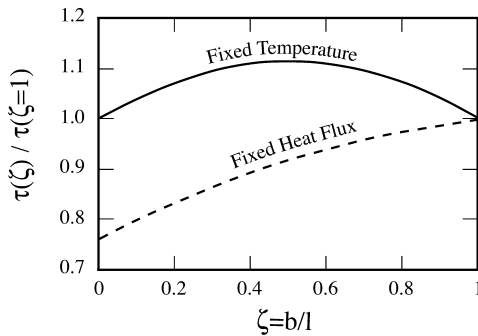


Fig. 4. Subsidence duration, τ_{90} (see text for definition), as a function of anomaly height for 1D thermal model. The subsidence time is scaled to the value for $\zeta=1$, corresponding to an anomaly at the base of the lithosphere.

amongst the four basins studied here, which amount to more than a factor of two, cannot be accounted for by differences of anomaly depth. We do not favour the explanations put forward by previous authors, which are to invoke different basal boundary conditions or large variations of lithosphere thickness [4,6,8]. A simpler hypothesis is to invoke deep lithospheric anomalies affecting the same lithosphere but with different widths.

3.3. Horizontal heat transport

For the boundary conditions of this problem, one may write the temperature perturbation as follows [26, pp. 33–35]:

$$\theta(r^*, z^*, t^*) = \theta_Z(z^*, t^*) \theta_R(r^*, t^*) \quad (13)$$

The vertical component, θ_Z , is the same as before and the radial component, θ_R , satisfies:

$$\theta_R(r^*, 0) = 1, \text{ for } r^* \leq 1 \quad (14)$$

$$\theta_R(r^*, 0) = 0, \text{ for } r^* > 1 \quad (15)$$

$$\theta_R(r^*, t^*) \rightarrow 0, \text{ as } r^* \rightarrow \infty \quad (16)$$

The corresponding solution is [26, p. 260]:

$$\theta_R(r^*, t^*) = \frac{\exp(-r^{*2}/4t^* \xi^2)}{2t^* \xi^2} \int_0^1 \exp\left(-\frac{r^{*2}}{4t^* \xi^2}\right) I_0\left(\frac{rr^*}{2t^*}\right) r dr \quad (17)$$

with I_0 the Bessel function of the first kind and order 0. For this solution, the size of the heated region next to the anomaly is small and temperatures there remain small at all times. At the centre

$$\theta_R(0, t^*) = 1 - \exp\left(-\frac{1}{4t^*} \xi^2\right) \quad (18)$$

which provides a simple measure of the acceleration of cooling due to horizontal heat loss. For thermal anomalies with elliptical or rectangular planforms, lateral heat transfer is dominated by the smallest horizontal dimension.

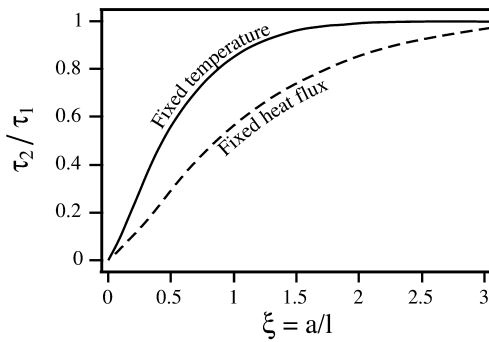


Fig. 5. The acceleration of subsidence as a function of anomaly width ξ for the two basal boundary conditions. The dimensionless anomaly depth, ζ , is set at 0.5. Acceleration is given as the ratio between the times needed to achieved 90% of the total subsidence in 2D and 1D models.

We denote by τ_1 and τ_2 the 1D and 2D values of the subsidence time τ_{90} respectively. Fig. 5 shows the ratio between these two times as a function of dimensionless anomaly radius. In the fixed flux case, horizontal heat losses remain important up to $a/l=3$. For the sake of example, Fig. 6 compares the Michigan basin subsidence record to the predicted thermal contraction with one particular 2D thermal model in the isostatic approximation.

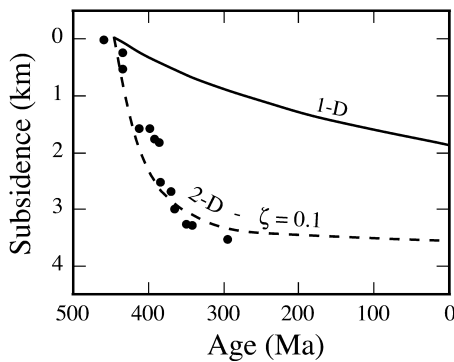


Fig. 6. Thermal model for subsidence in the Michigan basin for fixed basal heat flux. The lithosphere thickness is set at 300 km and the anomaly radius is 30 km. The curve predicted by a 1D model is given for comparison.

4. Deep lithospheric anomalies beneath intracratonic basins

4.1. Lithosphere thickness and anomaly width

For each basin, we first fix $\zeta=0.5$ and calculate the radius of the thermal anomaly which accounts for the observed subsidence time τ_{90} as a function of lithosphere thickness (Figs. 7 and 8). For very thick lithosphere, the subsidence time is much smaller than the vertical diffusion time-scale τ . In this case, cooling is achieved predominantly by horizontal heat loss and hence is mostly sensitive to the anomaly radius. For given subsidence time, the anomaly radius increases as the lithosphere thickness is decreased. With decreasing lithosphere thickness, the anomaly width tends towards infinity as the 1D cooling time tends towards the observed subsidence time. This defines the thinnest lithosphere which can account for the observations. This lower bound is a function of the basal boundary condition.

The Williston basin has the longest subsidence history and hence provides the most stringent constraint on lithosphere thickness. For fixed temperature at the base (Fig. 7), there is no solution for this basin if the lithosphere thickness is smaller than 200 km. For fixed heat flux (Fig. 8), lithospheres thinner than 125 km are ruled out. If we

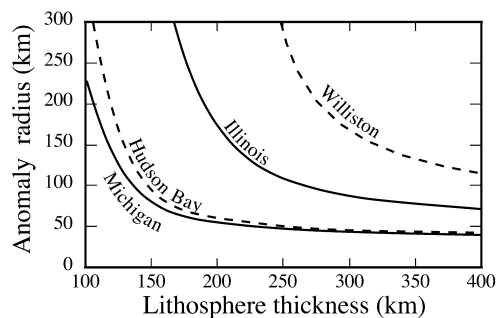


Fig. 7. Anomaly radius as a function of lithosphere thickness for fixed basal temperature and for $\zeta=0.5$. For each basin, the subsidence duration τ_{90} must be equal to the observed one. For large lithosphere thickness, lateral heat transport dominates and the anomaly radius is almost constant. For thin lithosphere, the anomaly radius increases as the time-scale for 1D thermal relaxation tends towards the observed subsidence time.

add the constraint that a/γ is less than 1.2, which was discussed above, values of the flexural parameter in Table 1 imply that a is smaller than about 160 km. This implies in turn that the lithosphere thickness is larger than 300 and 170 km for fixed temperature and fixed heat flux, respectively (Figs. 7 and 8).

For fixed lithosphere thickness, subsidence duration leads to an estimate of load radius a and hence, for given γ , to a predicted basin shape. All else being equal, the width of the anomaly is much smaller for the fixed heat flux model than for the fixed temperature one. This is because the 1D cooling time is much larger in the former model, which requires an enhancement of horizontal heat loss to achieve the same subsidence duration. Fig. 9 shows a cross-section through the present-day Williston basin, from [6], as well as the flexure profile predicted from the two thermal models for 250 km-thick lithosphere. The fixed temperature case requires too wide an anomaly and implies a basin floor which is much flatter than observed. The fixed heat flux case, however, provides a solution which is consistent with the observations. Furthermore, this case is the most realistic from a physical point of view because it accounts for the limited thermal efficiency of mantle convection. Models for lithosphere stabilisation rely on small-scale convection to provide the deep heat flux required for thermal steady-state [27,3]. In the fixed temperature solution, the mantle below the lithosphere is required to sustain a specific heat flux variation as a function of time.

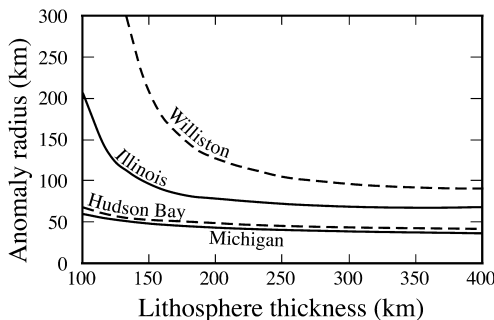


Fig. 8. Same as Fig. 7 for a fixed heat flux basal boundary condition.

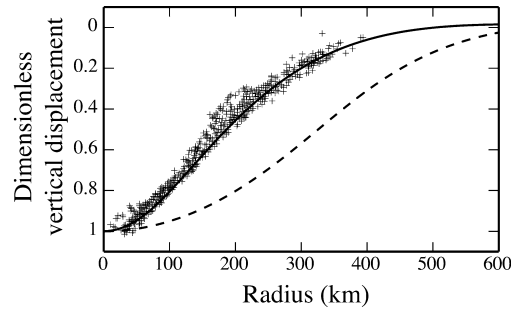


Fig. 9. Dimensionless surface displacement due to a deep lithospheric anomaly beneath the Williston basin. The plain and dashed curves correspond to the fixed flux and fixed temperature solutions for $l=250$ km. The crosses correspond to stacked sedimentary profiles from deep boreholes, from [6].

4.2. Anomaly depth and compositional density contrast

In the following, we fix the lithosphere thickness at 250 km, following [3]. The anomaly radius can be determined from the thermal model and hence the known value of point load Q_0 (Table 1) leads to an estimate of the load per unit area, P_0 . For an anomaly of height $H=l-b$, $P_0 = \Delta\rho_c g H$, where $\Delta\rho_c = \rho_m - \rho_l$ and ρ_l is the density of the continental lithosphere. For given H , the thermal model is run for the corresponding value of ζ to produce an estimate of the anomaly radius a . This leads to values for P_0 and $\Delta\rho_c$. The relationship between $\Delta\rho_c$ and H is illustrated in Fig. 10 for the Michigan basin.

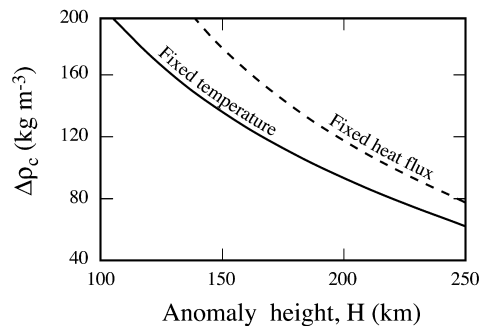


Fig. 10. Compositional density contrast in the deep lithospheric anomaly as a function of anomaly height. Parameters are those of the Michigan basin and the lithosphere thickness is set at 250 km.

Xenolith studies indicate that the magnitude of chemically induced density variations in the mantle part of the lithosphere may be as large as 110 kg m^{-3} [1]. Within this range, the value of 100 kg m^{-3} for $\Delta\rho_c$ allows a solution for all basins and is consistent with the magnitude of gravity anomalies (see below). We adopt this value and list results for the fixed heat flux thermal model only. For the Michigan basin, the anomaly height is 220 km and the associated radius is 50 km (Fig. 10). For the Williston basin, the longer subsidence history implies a wider anomaly, with 110 km radius and 105 km height.

We also use gravity anomalies to obtain an independent relationship between $\Delta\rho_c$ and H . Previous authors used thin and shallow disk loads [4,5], interpreted as dense crustal material due to phase changes, and adjusted the load radius in order to fit the observed gravity signal. Here, the load radius is constrained by the thermal model, and the same gravity signal can be generated by a narrow anomaly over a large height. In [5], a rough filtering procedure allows an estimate of about $+5 \text{ mgal}$ for the gravity anomaly above the Michigan basin. A global look at the four basins indicates that their net gravity anomalies are small, if they exist at all. To allow for errors in gravity analysis, we look for solutions such that the net anomaly is $0 \pm 10 \text{ mgal}$. We calculate the solution for a buried cylinder and keep the same density contrast of 100 kg m^{-3} . For the Michigan basin, we find that H must be larger than 210 km, which is consistent with the previous results. The half-width of the gravity anomaly is about 90 km, which is in agreement with observation [4,5].

5. Discussion

5.1. Lithospheric anomalies beneath the North American craton

Results for the four North American basins are illustrated in Fig. 11, for a lithosphere thickness of 250 km, fixed basal heat flux and $\Delta\rho_c = 100 \text{ kg m}^{-3}$. We found two types of anomalies: wide and thin for the Williston and Illinois basins, narrow and tall for the Michigan and Hudson Bay basins.

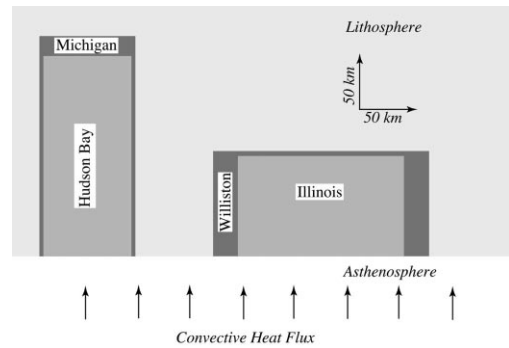


Fig. 11. Predicted shapes of deep lithospheric anomalies for four intracratonic basins of North America in 250 km thick lithosphere.

Interestingly, this grouping also corresponds to the onset of subsidence (Fig. 2), which occurred at the same age of about 520 Ma in the Williston and Illinois basins, in contrast to the younger age of about 460 Ma for the Michigan and Hudson Bay. The tall and narrow intrusion shape found here is very similar to a cylindrical anomaly detected beneath the Trans-Hudson Orogen, which has a radius and height of about 60 and 160 km, respectively [28].

Errors on these results arise from several sources. We equate the uncertainty on subsidence duration to the longest discontinuity in the sedimentation record, which amounts to about $\pm 10\%$. For the thermal model, this implies an error of $\pm 5\%$ on the anomaly width. The error on intrusion height is due to uncertainties on both the sedimentary load and intrusion width and the cumulative effect is about $\pm 20\%$. The same error affects the compositional density contrast estimate.

5.2. Plume penetration into the lithosphere?

The simplest explanation for intracratonic basins is the penetration of mantle plumes into the continental lithosphere. Current models have been developed for thin oceanic lithosphere, and thick continental lithosphere introduces important effects. Within the lower lithosphere, stresses at the top of the plume may drive significant local return flow, which reduces the amount of dynamic uplift. A key feature is that the density contrast

between plume material and surrounding continental mantle is the sum of compositional and thermal components, such that its net buoyancy is small initially, implying a small amount of surface uplift after emplacement. Further, the width and ascent rate of the flow are likely to depend on thermal structure and hence thickness of the lithosphere, with important implications for the evolution of plume temperature and decompression melting. Laboratory experiments and simple theoretical arguments on plume interaction with thick lithosphere have been developed to address these issues (Kaminski and Jaupart, 2000, in preparation). A complete test of the plume hypothesis is outside the scope of this paper and we only discuss two issues: the buoyancy required to drive plume penetration and the anomaly shape.

The compositional and thermal components of plume density, $\Delta\rho_c$ and $\Delta\rho_T$, are such that the former is positive and the latter negative. The present-day Hawaiian plume is about 300 K hotter than ‘normal’ convecting oceanic mantle [29]. Such a plume would need to rise first through the convective boundary layer at the base of the lithosphere, across which there is a temperature difference of about 200 K [3]. Thus, it would reach the base of the lithosphere with a temperature contrast of about 500 K. For a thermal expansion coefficient of $4 \times 10^{-5} \text{ K}^{-1}$ and an average mantle density of $3.5 \times 10^3 \text{ kg m}^{-3}$ at 250 km depth, $\Delta\rho_T \approx -70 \text{ kg m}^{-3}$. For the plume to rise through the continental lithospheric mantle, it must be buoyant with respect to it, i.e. such that $\Delta\rho_c + \Delta\rho_T < 0$. In the solutions above, $\Delta\rho_c \approx 100 \pm 20 \text{ kg m}^{-3}$, which is close to this requirement. The ‘cratonic’ plumes beneath North America could have been hotter than the Hawaiian plume. There may also be an additional load beneath the basins due to a small amount of phase change or of erosion. For example, a local crustal thinning of 4 km, which may exist under the Williston basin [17], would lower the deep lithospheric compositional density contrast to about $85 \pm 20 \text{ kg m}^{-3}$.

The two types of deep lithospheric anomalies (Fig. 11) may be explained in two different ways. One may envision plumes with different buoyancy fluxes, with the weaker ones being un-

able to penetrate deep into the lithosphere and pooling at its base. Alternatively, one may invoke plumes with different lifespans, with only the long-lived ones being able to affect the lithosphere over large thicknesses.

5.3. Subsidence analysis

In subsidence analysis, one must distinguish between thermal, tectonic, metamorphic and eustatic controls using the specific features of each one. For example, Bond and Kominz [30] rely on the assumption that the continental lithosphere has a characteristic cooling time of about 60 Myr, following the influential paper by Sleep [31]. Therefore, they attribute subsidence phases which last significantly longer than this to other effects, such as renewed tectonic activity for example. Such explanations are not warranted for thick continental lithosphere with large thermal response time, as illustrated in the present study.

6. Conclusion

Thermal models illustrate how the width of a deep lithospheric anomaly controls the time-scale of subsidence in thick lithosphere. It is not possible to account for subsidence data in the four intracratonic basins of North America if the lithosphere is thinner than 170 km. If the cratonic lithosphere is thick, the inevitable consequence is that the mantle part of the lithosphere must be compositionally buoyant with respect to the convective mantle below. In turn, this implies that the emplacement of deep mantle material into the lithosphere leads: (1) to a thermal anomaly inducing contraction and subsidence and (2) a permanent positive density contrast driving steady-state flexure. The dimensions of the deep lithospheric anomalies which underlie these basins should prove useful for investigating the physical mechanism of basin formation.

Acknowledgements

We thank Norman Sleep and two anonymous

reviewers for sensible comments which led to significant improvements of the manuscript. **[FA]**

References

- [1] T.H. Jordan, Continents as a chemical boundary layer, *Phil. Trans. R. Soc. London A* 301 (1981) 359–373.
- [2] S.P. Grand, Tomographic inversion for shear velocity beneath the North American plate, *J. Geophys. Res.* 92 (1987) 14065–14090.
- [3] C. Jaupart, J.-C. Mareschal, L. Guillou-Frottier, A. Davaille, Heat flow and thickness of the lithosphere in the Canadian Shield, *J. Geophys. Res.* 10 (1998) 15269–15286.
- [4] W.F. Haxby, D.L. Turcotte, J.M. Bird, Thermal and mechanical evolution of the Michigan basin, *Tectonophysics* 36 (1976) 57–75.
- [5] J.A. Nunn, N.H. Sleep, Thermal contraction and flexure of intracratonic basins: a three dimensional study of the Michigan Basin, *Geophys. J. R. Astron. Soc.* 79 (1984) 587–635.
- [6] J.L. Ahern, S.R. Mrkvicka, A mechanical and thermal model for the evolution of the Williston Basin, *Tectonics* 3 (1984) 79–102.
- [7] Y. Hamdani, J.-C. Mareschal, J. Arkani-Hamed, Phase change and thermal subsidence in intracontinental sedimentary basins, *Geophys. J. Int.* 106 (1991) 657–665.
- [8] Y. Hamdani, J.-C. Mareschal, J. Arkani-Hamed, Phase change and thermal subsidence of the Williston basin, *Geophys. J. Int.* 116 (1994) 585–597.
- [9] J.L. Ahern, P.J. Dikeou, Evolution of the lithosphere beneath the Michigan basin, *Earth Planet. Sci. Lett.* 95 (1989) 73–84.
- [10] T.D. Bechtel, D.W. Forsyth, V.L. Sharpton, R.A. Grieve, Variations in effective elastic thickness of the North American lithosphere, *Nature* 343 (1990) 636–638.
- [11] C. Pinet, C. Jaupart, J.-C. Mareschal, C. Gariépy, G. Bienfait, R. Lapointe, Heat flow and structure of the lithosphere in the eastern Canadian Shield, *J. Geophys. Res.* 96 (1991) 19,941–19,963.
- [12] S. Van der Lee, G. Nolet, Upper mantle *S* velocity structure of North America, *J. Geophys. Res.* 102 (1997) 22815–22838.
- [13] C.M.R. Fowler, E.G. Nisbet, The subsidence of the Williston basin, *Can. J. Earth Sci.* 22 (1985) 408–415.
- [14] G. Quinlan, Models of subsidence mechanisms in cratonic basins and their applicability to North-American examples, in: C. Beaumont, A. Tankard (Eds.), *Sedimentary Basins and Basin forming Mechanisms*, Canadian Society of Petroleum Geologists Memoir 12, 1987, pp. 463–481.
- [15] A.M. Stueber, L.M. Walter, Glacial recharge and paleo-hydrological flow systems in the the Illinois basin: evidence from chemistry of Ordovician carbonates (Galena) formation waters, *Geol. Soc. Am. Bull.* 106 (1994) 1430–1439.
- [16] B.V. Sanford, Paleozoic geology of the hudsonian platform, in: C. Beaumont, A. Tankard (Eds.), *Sedimentary Basins and Basin forming Mechanisms*, Canadian Society of Petroleum Geologists Memoir 12, 1987, pp. 483–505.
- [17] P. Morel-à-l’Huissier, A.G. Green, C.J. Pike, Crustal refraction surveys across the Trans-Hudson orogen/Williston basin of south-central Canada, *J. Geophys. Res.* 92 (1987) 6403–6420.
- [18] T. Zhu, L.D. Brown, Consortium for continental reflection profiling Michigan surveys: reprocessing and results, *J. Geophys. Res.* 91 (1986) 11477–11495.
- [19] R.L. Rudnick, D.M. Fountain, Nature and composition of the continental crust: a lower crustal perspective, *Rev. Geophys.* 33 (1995) 267–309.
- [20] M.F. Middleton, A model of intracratonic basin formation entailing deep crustal metamorphism, *Geophys. J. R. Astron. Soc.* 62 (1980) 1–14.
- [21] M.-P. Doin, L. Fleitout, D. McKenzie, Geoid anomalies and the structure of continental and oceanic lithospheres, *J. Geophys. Res.* 101 (1996) 16119–16136.
- [22] N.H. Sleep, Platform subsidence mechanisms and ‘eustatic’ sea-level changes, *Tectonophysics* 36 (1976) 45–56.
- [23] J.F. Brotchie, R. Sylvester, On crustal flexure, *J. Geophys. Res.* 22 (1969) 5240–5252.
- [24] M. Abramowitz, I.A. Stegun, *Handbook of Mathematical Functions*, United States Department of Commerce, Washington, DC, 1964.
- [25] W.J. Hinze, J.W. Bradley, A.R. Brown, Gravimeter survey in the Michigan basin deep borehole, *J. Geophys. Res.* 83 (1978) 5864–5868.
- [26] H.S. Carslaw, J.C. Jaeger, *Conduction of Heat in Solids*, 2nd edn., Oxford Science Publications, Oxford, 1959.
- [27] A. Davaille, C. Jaupart, Transient high-Rayleigh-number thermal convection with large viscosity variations, *J. Fluid Mech.* 253 (1993) 141–166.
- [28] C.G. Bank, M.G. Bostock, R.M. Ellis, Z. Hajnal, J.C. VanDecar, Lithospheric mantle structure beneath the Trans-Hudson Orogen and the origin of diamondiferous kimberlites, *J. Geophys. Res.* 103 (1998) 10103–10114.
- [29] N.M. Ribe, U.R. Christensen, The dynamical origin of Hawaiian volcanism, *Earth Planet. Sci. Lett.* 101 (1999) 517–531.
- [30] G.C. Bond, M.A. Kominz, Disentangling middle Paleozoic sea level and tectonic events in cratonic margins and cratonic basins of North America, *J. Geophys. Res.* 94 (1991) 6619–6639.
- [31] N.H. Sleep, Thermal effects of the formation of Atlantic continental margins by continental break-up, *Geophys. J. R. Astron. Soc.* 24 (1971) 325–350.